DAFTAR PUSTAKA

[1] L. Cheng *et al.*, "Osteoinduction of hydroxyapatite/β-tricalcium phosphate bioceramics in mice with a fractured fibula," *Acta Biomater.*, vol. 6, no. 4, pp. 1569–1574, 2010, doi: 10.1016/j.actbio.2009.10.050.

[2] Y. Zeng, J. Hoque, and S. Varghese, "Biomaterial-assisted local and systemic delivery of bioactive agents for bone repair," *Acta Biomater.*, vol. 93, no. January, pp. 152–168, 2019, doi: 10.1016/j.actbio.2019.01.060.

[3] P. Terzioğlu, H. Öğüt, and A. Kalemtaş, "Natural calcium phosphates from fish bones and their potential biomedical applications," *Mater. Sci. Eng. C*, vol. 91, pp. 899–911, 2018, doi: 10.1016/j.msec.2018.06.010.

[4] A. Elkayar, Y. Elshazly, and M. Assaad, "properties of Hydroxyapatite from Bovine Teeth," 2009. [Online]. Available: http://www.la-press.com.http//www.la-press.com.

[5] K. Madhumathi *et al.*, "Wet chemical synthesis of chitosan hydrogel-hydroxyapatite composite membranes for tissue engineering applications," *Int. J. Biol. Macromol.*, vol. 45, no. 1, pp. 12–15, 2009, doi: 10.1016/j.ijbiomac.2009.03.011.

[6] K. S. Vecchio, X. Zhang, J. B. Massie, M. Wang, and C. W. Kim, "Conversion of bulk seashells to biocompatible hydroxyapatite for bone implants," *Acta Biomater.*, vol. 3, no. 6, pp. 910–918, 2007, doi: 10.1016/j.actbio.2007.06.003.

[7] X. Huang, Y. Huang, Z. Ouyang, and Q. Qin, "Establishment of a cell line from the brain of grouper (Epinephelus akaara) for cytotoxicity testing and virus pathogenesis," *Aquaculture*, vol. 311, no. 1–4, pp. 65–73, 2011, doi: 10.1016/j.aquaculture.2010.11.037.

[8] T. M. Coelho, "Characterization of natural nanostructured hydroxyapatite obtained from the bones of Brazilian river fish," *J. Appl. Phys.*, vol. 100, no. 9, 2006, doi: 10.1063/1.2369647.

[9] M. Wang *et al.*, "Synthesis and characterization of an injectable and self-curing poly(methyl methacrylate) cement functionalized with a biomimetic

chitosan-poly(vinyl alcohol)/nano-sized hydroxyapatite/silver hydrogel," *RSC Adv.*, vol. 6, no. 65, pp. 60609–60619, 2016, doi: 10.1039/c6ra08182g.

[10] J. Y. Park, Y. H. Kim, J. H. Kim, and I. C. Bang, "The complete mitochondrial genome of the hybrid grouper Epinephelus fuscoguttatus (♀) × E. polyphekadion (♂)," *Mitochondrial DNA Part B Resour.*, vol. 5, no. 3, pp. 3283–3284, 2020, doi: 10.1080/23802359.2020.1812447.

[11] K. Kuriiwa, S. N. Chiba, H. Motomura, and K. Matsuura, "Phylogeography of Blacktip Grouper, Epinephelus fasciatus (Perciformes: Serranidae), and influence of the Kuroshio Current on cryptic lineages and genetic population structure," *Ichthyol. Res.*, vol. 61, no. 4, pp. 361–374, 2014, doi: 10.1007/s10228-014-0408-9.

[12] M. Boutinguiza, J. Pou, R. Comesaña, F. Lusquiños, A. De Carlos, and B. León, "Biological hydroxyapatite obtained from fish bones," *Mater. Sci. Eng. C*, vol. 32, no. 3, pp. 478–486, 2012, doi: 10.1016/j.msec.2011.11.021.

[13] M. Sadat-Shojai, M. T. Khorasani, E. Dinpanah-Khoshdargi, and A. Jamshidi, "Synthesis methods for nanosized hydroxyapatite with diverse structures," *Acta Biomaterialia*, vol. 9, no. 8. Elsevier Ltd, pp. 7591–7621, 2013. doi: 10.1016/j.actbio.2013.04.012.

[14] G. Aydin, P. Terzioğlu, H. Öğüt, and A. Kalemtas, "Production, characterization, and cytotoxicity of calcium phosphate ceramics derived from the bone of meagre fish, Argyrosomus regius," *J. Aust. Ceram. Soc.*, vol. 57, no. 1, pp. 37–46, 2021, doi: 10.1007/s41779-020-00513-w.

[15] Y. H. Tseng, C. S. Kuo, Y. Y. Li, and C. P. Huang, "Polymer-assisted synthesis of hydroxyapatite nanoparticle," *Mater. Sci. Eng. C*, vol. 29, no. 3, pp. 819–822, 2009, doi: 10.1016/j.msec.2008.07.028.

[16] S. K. Swain, S. Bhattacharyya, and D. Sarkar, "Fabrication of porous hydroxyapatite scaffold via polyethylene glycol-polyvinyl alcohol hydrogel state," *Mater. Res. Bull.*, vol. 64, pp. 257–261, 2015, doi: 10.1016/j.materresbull.2014.12.072.

[17] M. C. Chang, B. G. Kim, and J. H. Whang, "Compressive strength enhancement of artificial bone using hydroxyapatite/fish-collagen

nanocomposite," *J. Korean Ceram. Soc.*, vol. 57, no. 3, pp. 321–330, 2020, doi: 10.1007/s43207-020-00026-z.

[18] B. Mondal, S. Mondal, A. Mondal, and N. Mandal, "Fish scale derived hydroxyapatite scaffold for bone tissue engineering," *Mater. Charact.*, vol. 121, pp. 112–124, 2016, doi: 10.1016/j.matchar.2016.09.034.

[19] A. Pal, S. Paul, A. R. Choudhury, V. K. Balla, M. Das, and A. Sinha, "Synthesis of hydroxyapatite from Lates calcarifer fish bone for biomedical applications," *Mater. Lett.*, vol. 203, pp. 89–92, 2017, doi: 10.1016/j.matlet.2017.05.103.

[20] P. Kumar, B. Vinitha, and G. Fathima, "Bone grafts in dentistry," *J. Pharm. Bioallied Sci.*, vol. 5, no. SUPPL.1, pp. 125–128, 2013, doi: 10.4103/0975-7406.113312.

[21] A. Z. Alshemary, M. Akram, A. Taha, A. Tezcaner, Z. Evis, and R. Hussain, "Physico-chemical and biological properties of hydroxyapatite extracted from chicken beaks," *Mater. Lett.*, vol. 215, pp. 169–172, 2018, doi: 10.1016/j.matlet.2017.12.076.

[22] W. Chen *et al.*, "Characterization of microRNAs in orange-spotted grouper (Epinephelus coioides) fin cells upon red-spotted grouper nervous necrosis virus infection," *Fish Shellfish Immunol.*, vol. 63, pp. 228–236, 2017, doi: 10.1016/j.fsi.2017.02.031.

[23] Q. Wang *et al.*, "Molecular identification of GnIH/GnIHR signal and its reproductive function in protogynous hermaphroditic orange-spotted grouper (Epinephelus coioides)," *Gen. Comp. Endocrinol.*, vol. 216, pp. 9–23, 2015, doi: 10.1016/j.ygcen.2015.04.016.

[24] J. Huang, G. Chen, Z. Wang, and J. Zhang, "Use of response surface methodology to study the combined effects of temperature and salinity on hatching and deformity of the hybrid grouper, Epinephelus fuscoguttatus (♀) × Epinephelus polyphekadion (♂)," *Aquac. Res.*, vol. 49, no. 5, pp. 1997–2005, 2018, doi: 10.1111/are.13655.

[25] E. Amenyogbe, G. Chen, and Z. Wang, "Identification, characterization, and expressions profile analysis of growth hormone receptors (GHR1 and

GHR2) in Hybrid grouper (Epinephelus fuscoguttatus ♀ × Epinephelus polyphekadion ♂)," *Genomics*, vol. 112, no. 1, pp. 1–9, 2020, doi: 10.1016/j.ygeno.2019.05.012.

[26] S. R. Dutta, D. Passi, P. Singh, and A. Bhuibhar, "Ceramic and non-ceramic hydroxyapatite as a bone graft material: a brief review," *Ir. J. Med. Sci.*, vol. 184, no. 1, pp. 101–106, 2015, doi: 10.1007/s11845-014-1199-8.

[27] H. Denissen, R. Martinetti, A. Van Lingen, and A. Van Den Hooff, "Normal Osteoconduction and Repair," vol. 71, no. 2.

[28] D. S. Seo and J. K. Lee, "Dissolution of human teeth-derived hydroxyapatite," *Ann. Biomed. Eng.*, vol. 36, no. 1, pp. 132–140, Jan. 2008, doi: 10.1007/s10439-007-9394-7.

[29] D. V. Abere, S. A. Ojo, G. M. Oyatogun, M. B. Paredes-Epinosa, M. C. D. Niluxsshun, and A. Hakami, "Mechanical and morphological characterization of nano-hydroxyapatite (nHA) for bone regeneration: A mini review," *Biomed. Eng. Adv.*, vol. 4, no. June, p. 100056, 2022, doi: 10.1016/j.bea.2022.100056.

[30] R. A. Rahmat, M. A. Humphries, J. J. Austin, A. M. T. Linacre, and P. Self, "The development of a tool to predict temperature-exposure of incinerated teeth using colourimetric and hydroxyapatite crystal size data," *Int. J. Legal Med.*, vol. 135, no. 5, pp. 2045–2053, Sep. 2021, doi: 10.1007/s00414-021-02538-7.

[31] G. Halim, E. M. Setiawatie, N. Ulfah, R. I. Permatasari, and B. Manafe, "Cytotoxicity evaluation of bovine tooth hydroxyapatite," in *AIP Conference Proceedings*, Dec. 2020, vol. 2314. doi: 10.1063/5.0036493.

[32] S. L. Bee and Z. A. A. Hamid, "Characterization of chicken bone waste-derived hydroxyapatite and its functionality on chitosan membrane for guided bone regeneration," *Compos. Part B Eng.*, vol. 163, no. January, pp. 562–573, 2019, doi: 10.1016/j.compositesb.2019.01.036.

[33] P. Bunlipatanon, N. Songseechan, H. Kongkeo, N. W. Abery, and S. S. De Silva, "Comparative efficacy of trash fish versus compounded commercial feeds in cage aquaculture of Asian seabass (Lates calcarifer) (Bloch) and

tiger grouper (Epinephelus fuscoguttatus) (Forsskål)," *Aquac. Res.*, vol. 45, no. 3, pp. 373–388, 2014, doi: 10.1111/j.1365-2109.2012.03234.x.

[34] N. Mustafa, M. H. I. Ibrahim, R. Asmawi, and A. M. Amin, "Hydroxyapatite Extracted from Waste Fish Bones and Scales via Calcination Method," *Appl. Mech. Mater.*, vol. 773–774, pp. 287–290, 2015, doi: 10.4028/www.scientific.net/amm.773-774.287.

[35] P. V. Nam, N. Van Hoa, and T. S. Trung, "Properties of hydroxyapatites prepared from different fish bones: A comparative study," *Ceram. Int.*, vol. 45, no. 16, pp. 20141–20147, 2019, doi: 10.1016/j.ceramint.2019.06.280.

[36] M. de Azevedo e Sousa Munhoz *et al.*, "Elastin-derived scaffolding associated or not with bone morphogenetic protein (BMP) or hydroxyapatite (HA) in the repair process of metaphyseal bone defects," *PLoS One*, vol. 15, no. 4, pp. 1–21, 2020, doi: 10.1371/journal.pone.0231112.

[37] D. Wu *et al.*, "Hydroxyapatite-anchored dendrimer for in situ remineralization of human tooth enamel," *Biomaterials*, vol. 34, no. 21, pp. 5036–5047, Jul. 2013, doi: 10.1016/j.biomaterials.2013.03.053.

[38] B. Mondal, "Fish scale derived hydroxyapatite scaffold for bone tissue engineering," *Mater. Charact.*, vol. 121, pp. 112–124, 2016, doi: 10.1016/j.matchar.2016.09.034.

[39] T. Liu *et al.*, "K+/Sr2+/Na+ triple-doped hydroxyapatites/GelMA composite hydrogel scaffold for the repair of bone defects," *Ceram. Int.*, vol. 47, no. 21, pp. 30929–30937, 2021, doi: 10.1016/j.ceramint.2021.07.277.

[40] Y. Yang *et al.*, "Synthesis of aligned porous polyethylene glycol/silk fibroin/hydroxyapatite scaffolds for osteoinduction in bone tissue engineering," *Stem Cell Res. Ther.*, vol. 11, no. 1, pp. 1–17, 2020, doi: 10.1186/s13287-020-02024-8.

[41] Z. L. Ou-Yang *et al.*, "Establishment and characterization of a new marine fish cell line derived from red-spotted grouper Epinephelus akaara," *J. Fish Biol.*, vol. 77, no. 5, pp. 1083–1095, 2010, doi: 10.1111/j.1095-

8649.2010.02749.x.

[42] N. M. Ergul *et al.*, “3D printing of chitosan/ poly(vinyl alcohol) hydrogel containing synthesized hydroxyapatite scaffolds for hard-tissue engineering,” *Polym. Test.*, vol. 79, p. 106006, 2019, doi: 10.1016/j.polymertesting.2019.106006.

[43] M. I. Baker, S. P. Walsh, Z. Schwartz, and B. D. Boyan, “A review of polyvinyl alcohol and its uses in cartilage and orthopedic applications,” *J. Biomed. Mater. Res. - Part B Appl. Biomater.*, vol. 100 B, no. 5, pp. 1451–1457, 2012, doi: 10.1002/jbm.b.32694.

[44] M. J. Kim, S. H. Lee, N. Y. Lee, and I. H. Lee, “Evaluation of the effect of PVA tape supplemented with 2.26% fluoride on enamel demineralization using microhardness assessment and scanning electron microscopy: In vitro study,” *Arch. Oral Biol.*, vol. 58, no. 2, pp. 160–166, 2013, doi: 10.1016/j.archoralbio.2012.06.015.

[45] T. Wang, J. Wu, Y. Yi, and J. Qi, “Optimization of Process Conditions for Infected Animal Tissues by Alkaline Hydrolysis Technology,” *Procedia Environ. Sci.*, vol. 31, pp. 366–374, 2016, doi: 10.1016/J.PROENV.2016.02.049.

[46] L. Ho Khanh Hy, D. Viet Ha, P. Xuan Ky, N. Phuong Anh, P. Bao Vy, and D. Thi Thiet, “Preparation of Nano-hydroxyapatite Obtained from Lates Calcarifer Fish Bone by Alkaline Hydrolysis Method,” *Am. J. Chem. Biochem. Eng.*, vol. 5, no. 1, p. 32, 2021, doi: 10.11648/j.ajcbe.20210501.15.

[47] N. A. M. Barakat *et al.*, “Physiochemical characterizations of hydroxyapatite extracted from bovine bones by three different methods: Extraction of biologically desirable HAp,” *Mater. Sci. Eng. C*, vol. 28, no. 8, pp. 1381–1387, 2008, doi: 10.1016/j.msec.2008.03.003.

[48] Ò. Boronat *et al.*, “Development of added-value culinary ingredients from fish waste: Fish bones and fish scales,” *Int. J. Gastron. Food Sci.*, vol. 31, no. December 2022, pp. 0–6, 2023, doi: 10.1016/j.ijgfs.2022.100657.

[49] A. Przekora *et al.*, “Osteoclast-mediated acidic hydrolysis of thermally

gelled curdlan component of the bone scaffolds: Is it possible?," *Carbohydr. Polym.*, vol. 295, no. March, p. 119914, 2022, doi: 10.1016/j.carbpol.2022.119914.

[50] J. Venkatesan *et al.*, "Isolation and characterization of nano-hydroxyapatite from salmon fish bone," *Materials (Basel).*, vol. 8, no. 8, pp. 5426–5439, 2015, doi: 10.3390/ma8085253.

[51] X. Zheng *et al.*, "Remediation of Cd-, Pb-, Cu-, and Zn-contaminated soil using cow bone meal and oyster shell meal," *Ecotoxicol. Environ. Saf.*, vol. 229, p. 113073, 2022, doi: 10.1016/j.ecoenv.2021.113073.

[52] M. Saiful Firdaus Hussin, M. Izwana Idris, H. Zuhudi Abdullah, W. Azeem, and I. Ghazali, "Characterization and in vitro evaluation of hydroxyapatite from Fringescale sardinella bones for biomedical applications," *J. Saudi Chem. Soc.*, vol. 27, no. 5, p. 101721, 2023, doi: 10.1016/j.jscs.2023.101721.

[53] A. F. A. Latif, "Extraction of biological hydroxyapatite from tuna fish bone for biomedical applications," *Mater. Sci. Forum*, vol. 1010, pp. 584–589, 2020, doi: 10.4028/www.scientific.net/MSF.1010.584.

[54] Y. Pan *et al.*, "Injectable hydrogel-loaded nano-hydroxyapatite that improves bone regeneration and alveolar ridge promotion," *Mater. Sci. Eng. C*, vol. 116, no. March, p. 111158, 2020, doi: 10.1016/j.msec.2020.111158.

[55] S. Chen, Y. Shi, X. Zhang, and J. Ma, "3D printed hydroxyapatite composite scaffolds with enhanced mechanical properties," *Ceram. Int.*, vol. 45, no. 8, pp. 10991–10996, 2019, doi: 10.1016/j.ceramint.2019.02.182.

[56] P. Surya, A. Nithin, A. Sundaramanickam, and M. Sathish, "Synthesis and characterization of nano-hydroxyapatite from Sardinella longiceps fish bone and its effects on human osteoblast bone cells," *J. Mech. Behav. Biomed. Mater.*, vol. 119, no. November 2020, p. 104501, 2021, doi: 10.1016/j.jmbbm.2021.104501.

[57] M. Mudhafar, "PREPARATION AND CHARACTERIZATION OF

BEADS OF FISH SCALES HYDROXYAPATITE/COLLAGEN /SILVER NANOPARTICLES BY USING INFILTRATION METHOD," *Malaysian J. Microsc.*, vol. 17, no. 2, pp. 239–250, 2021.

[58] T. Goto, "Effects of trace elements in fish bones on crystal characteristics of hydroxyapatite obtained by calcination," *Ceram. Int.*, vol. 40, no. 7, pp. 10777–10785, 2014, doi: 10.1016/j.ceramint.2014.03.067.

[59] M. Wojasiński, J. Latocha, P. Liszewska, Ł. Makowski, P. Sobieszuk, and T. Ciach, "Scaled-Up 3D-Printed Reactor for Precipitation of Lecithin-Modified Hydroxyapatite Nanoparticles," *Ind. Eng. Chem. Res.*, vol. 60, no. 35, pp. 12944–12955, 2021, doi: 10.1021/acs.iecr.1c02973.

[60] M. T. Hooi, "FTIR spectroscopy characterization and critical comparison of poly(vinyl)alcohol and natural hydroxyapatite derived from fish bone composite for bone-scaffold," *J. Phys. Conf. Ser.*, vol. 2120, no. 1, 2021, doi: 10.1088/1742-6596/2120/1/012004.

[61] P. Deb, E. Barua, S. Das Lala, and A. B. Deoghare, "Synthesis of hydroxyapatite from Labeo rohita fish scale for biomedical application," *Mater. Today Proc.*, vol. 15, pp. 277–283, 2019, doi: 10.1016/j.matpr.2019.05.006.

LAMPIRAN

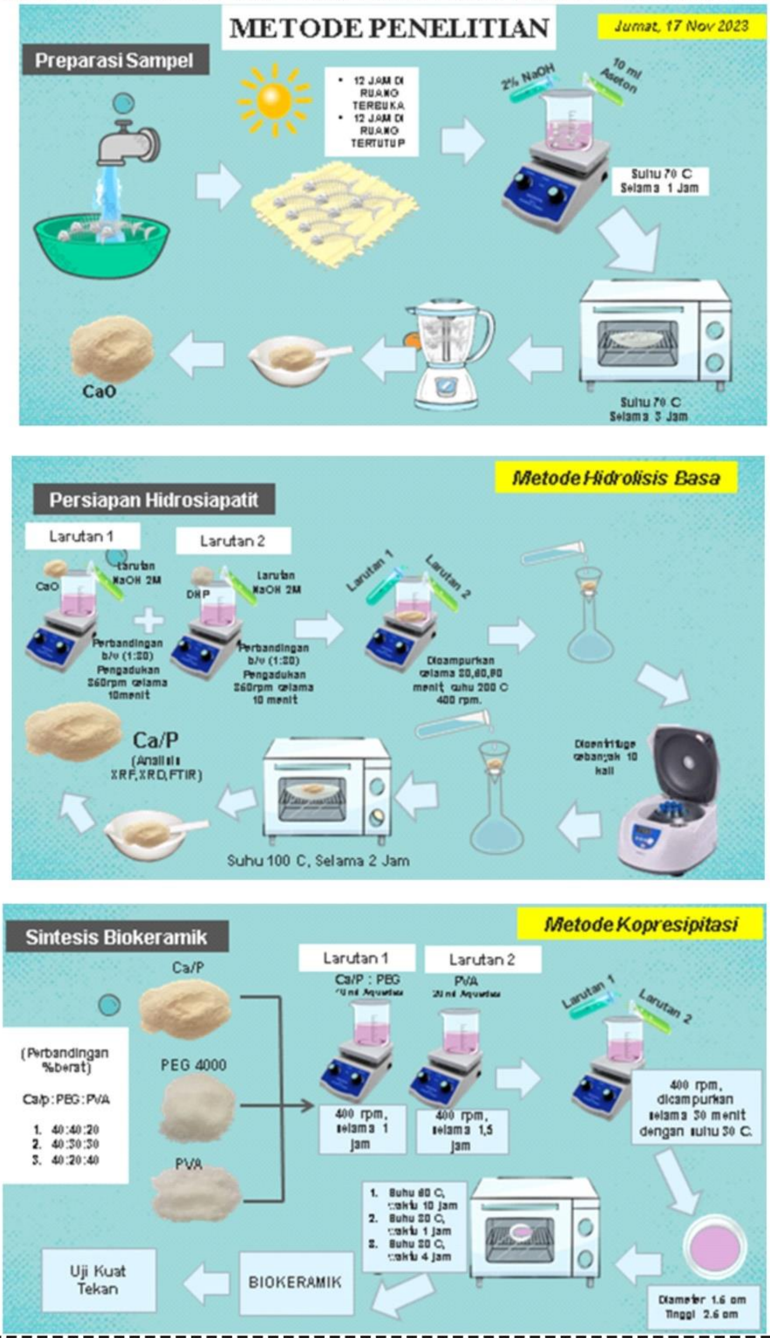
METODE PENELITIAN
Jumat, 17 Nov 2023
Preparasi Sampel
• 12 JAM DI RUANG TERBUKA
• 12 JAM DI RUANG TERTUTUP
2% NaOH
10 ml Aseton
Suhu 70 C Selama 1 Jam
Suhu 70 C Selama 3 Jam
CaO
Metode Hidrolisis Basa
Persiapan Hidrosiapatit
Larutan 1
Larutan 2
CaO
Larutan NaOH 2M
DHP
Larutan NaOH 2M
Perbandingan b/v (1:20) Pengadukan 360rpm selama 10menit
Perbandingan b/v (1:20) Pengadukan 360rpm selama 10 menit
Larutan 1
Larutan 2
Dicampurkan selama 30,60,90 menit, suhu 200 C 400 rpm.
Dicentrifuge sebanyak 10 kali
Ca/P
(Analisis XRF,XRD,FTIR)
Suhu 100 C, Selama 2 Jam
Metode Kopresipitasi
Sintesis Biokeramik
Ca/P
PEG 4000
PVA
(Perbandingan %berat)
Ca/p : PEG : PVA
1. 40:40:20
2. 40:30:30
3. 40:20:40
Larutan 1
Ca/P : PEG
Larutan 2
PVA
400 rpm, selama 1 jam
400 rpm, selama 1,5 jam
Larutan 1
Larutan 2
400 rpm, dicampurkan selama 30 menit dengan suhu 30 C.
Diameter 1.6 cm Tinggi 2.6 cm
1. Suhu 60 C, waktu 10 jam
2. Suhu 30 C, waktu 1 jam
3. Suhu 30 C, waktu 4 jam
BIOKERAMIK
Uji Kuat Tekan

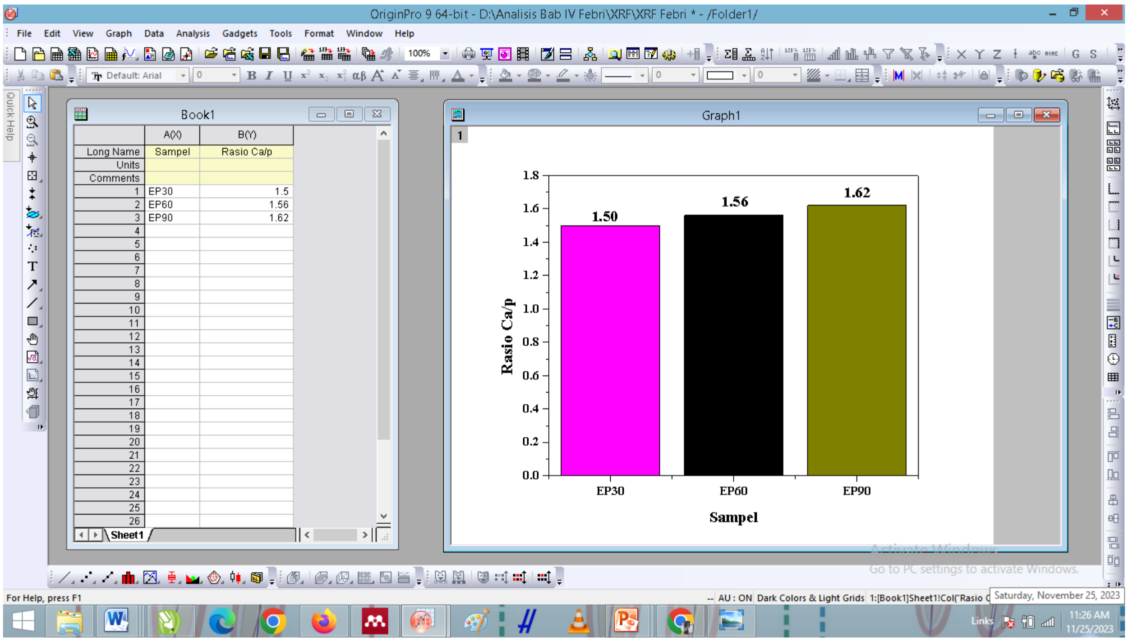
OriginPro 9 64-bit - D:\Analisis Bab IV Febri\XRF\XRF Febri * - /Folder1/
Book1
Long Name
Units
Comments
Sampel
Rasio Ca/p
EP30 1.5
EP60 1.56
EP90 1.62
Graph1
Rasio Ca/p
Sampel
1.50
1.56
1.62
EP30
EP60
EP90

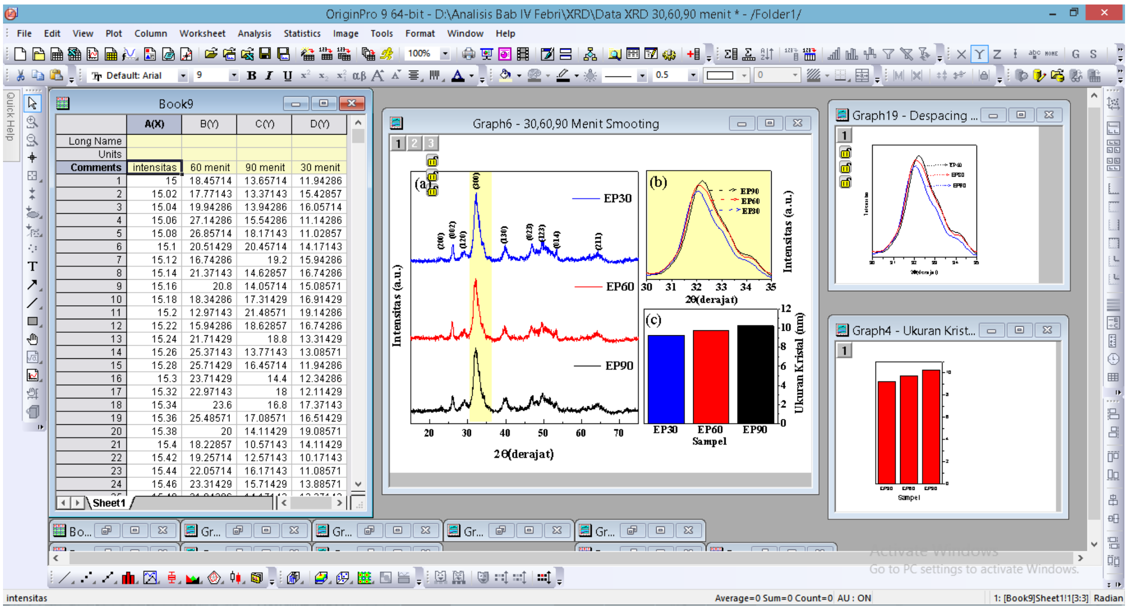
OriginPro 9 64-bit - D:\Analisis Bab IV Febri\XRD\Data XRD 30,60,90 menit * - /Folder1/
Book9
Graph6 - 30,60,90 Menit Smooting
Graph19 - Despacing ...
Graph4 - Ukuran Krist...
intensitas
60 menit
90 menit
30 menit
EP30
EP60
EP90
Intensitas (a.u.)
2θ(derajat)
Ukuran Kristal (nm)
Sampel

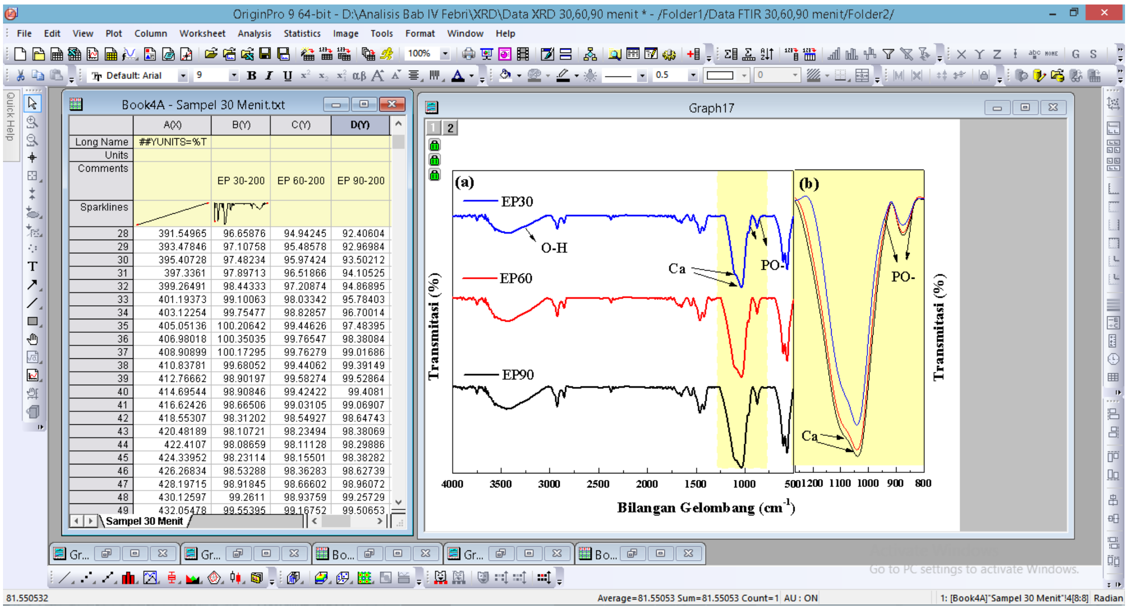
OriginPro 9 64-bit - D:\Analisis Bab IV Febri\XRD\Data XRD 30,60,90 menit * - /Folder1/Data FTIR 30,60,90 menit/Folder2/
Book4A - Sampel 30 Menit.txt
Graph17
EP 30-200
EP 60-200
EP 90-200
(a)
(b)
EP30
EP60
EP90
O-H
Ca
PO-
Transmitasi (%)
Bilangan Gelombang (cm-1)

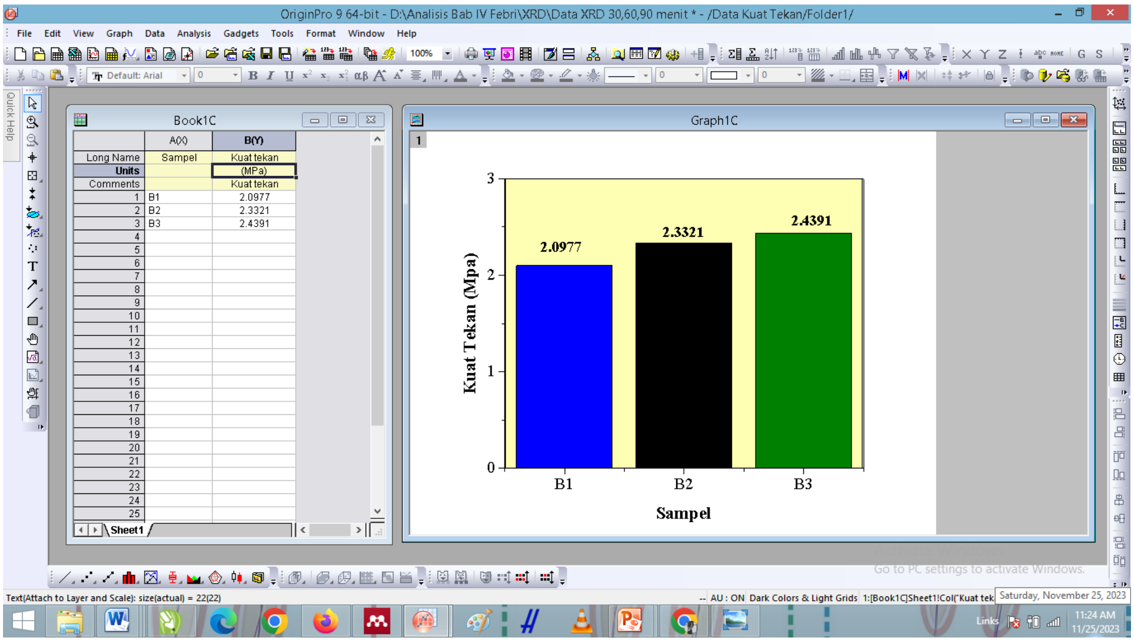
OriginPro 9 64-bit - D:\Analisis Bab IV Febri\XRD\Data XRD 30,60,90 menit * - /Data Kuat Tekan/Folder1/
Book1C
Long Name Sampel Kuat tekan
Units (MPa)
Comments Kuat tekan
1 B1 2.0977
2 B2 2.3321
3 B3 2.4391
Graph1C
2.0977
2.3321
2.4391
Kuat Tekan (Mpa)
B1
B2
B3
Sampel

Data XRD EP30

Strongest 3 peaks

no.	peak no.	2Theta (deg)	d (A)	I/I1	FWHM (deg)	Intensity (Counts)	Integrated Int (Counts)
1	5	32.3700	2.76351	100	1.58000	136	11234
2	14	49.7100	1.83264	24	0.94000	32	2134
3	2	26.0300	3.42042	23	0.62000	31	991

Peak Data List

peak no.	2Theta (deg)	d (A)	I/I1	FWHM (deg)	Intensity (Counts)	Integrated Int (Counts)
1	23.0500	3.85544	4	0.62000	6	244
2	26.0300	3.42042	23	0.62000	31	991
3	28.9800	3.07860	11	0.96000	15	664
4	29.5800	3.01751	6	0.92000	8	352
5	32.3700	2.76351	100	1.58000	136	11234
6	34.3600	2.60788	17	0.49340	23	1097
7	35.8200	2.50486	4	0.08000	5	67
8	39.8800	2.25871	21	1.04000	28	1557
9	41.1200	2.19341	3	0.56000	4	206
10	42.1400	2.14265	4	0.24000	5	131
11	44.0500	2.05407	4	0.38000	6	157
12	46.9350	1.93432	19	0.89000	26	1481
13	48.1400	1.88867	9	0.00000	12	0
14	49.7100	1.83264	24	0.94000	32	2134
15	50.7000	1.79915	14	0.00000	19	0
16	51.3600	1.77757	11	0.00000	15	0
17	52.2600	1.74905	10	0.48000	13	722
18	53.3000	1.71735	12	0.56000	16	535
19	56.2200	1.63488	3	0.28000	4	112
20	61.9100	1.49758	4	0.50000	5	199
21	63.0200	1.47384	5	0.28000	7	129
22	64.2100	1.44937	10	1.02000	14	700
23	65.0400	1.43287	7	0.52000	10	298
24	65.9700	1.41490	3	0.22000	4	67
25	72.5800	1.30146	4	0.24000	5	143
26	74.1700	1.27745	3	0.54000	4	110
27	74.7800	1.26853	3	0.68000	4	109

Data XRD EP60

Strongest 3 peaks

no.	peak no.	2Theta (deg)	d (A)	I/I1	FWHM (deg)	Intensity (Counts)	Integrated Int (Counts)
1	5	32.3266	2.76712	100	1.66670	131	9659
2	2	26.0250	3.42107	23	0.69000	30	1109
3	6	34.0000	2.63466	23	1.08000	30	2093

Peak Data List

peak no.	2Theta (deg)	d (A)	I/I1	FWHM (deg)	Intensity (Counts)	Integrated Int (Counts)
1	22.9900	3.86537	5	0.90000	6	360
2	26.0250	3.42107	23	0.69000	30	1109
3	29.1100	3.06515	14	1.14000	18	1277
4	30.9400	2.88790	15	0.60000	20	875
5	32.3266	2.76712	100	1.66670	131	9659
6	34.0000	2.63466	23	1.08000	30	2093
7	35.5300	2.52463	6	0.34000	8	229
8	39.8400	2.26088	19	1.32000	25	1800
9	42.3200	2.13395	4	0.16000	5	100
10	43.7900	2.06566	3	0.14000	4	87
11	46.8900	1.93607	18	0.98000	24	997
12	47.9000	1.89757	8	1.44000	11	744
13	49.6000	1.83644	21	0.96000	28	1708
14	50.6800	1.79981	13	0.00000	17	0
15	51.3400	1.77821	11	0.00000	14	0
16	51.8800	1.76097	9	1.36000	12	769
17	53.3300	1.71646	11	0.62000	14	469
18	56.1800	1.63595	4	0.48000	5	230
19	60.0900	1.53851	4	0.14000	5	110
20	61.7466	1.50115	5	0.33330	6	139
21	63.1000	1.47217	5	0.52000	7	260
22	64.1100	1.45139	10	0.86000	13	626
23	65.1100	1.43149	7	0.30000	9	235
24	66.0300	1.41376	3	0.18000	4	79
25	71.7000	1.31526	5	0.44000	6	273

Data XRD EP90

Strongest 3 peaks

no.	peak no.	2Theta (deg)	d (A)	I/I1	FWHM (deg)	Intensity (Counts)	Integrated Int (Counts)
1	6	32.0200	2.79291	100	1.21600	121	6131
2	7	33.0200	2.71058	52	0.92000	63	2576
3	2	25.9266	3.43383	26	0.61330	31	1028

Peak Data List

peak no.	2Theta (deg)	d (A)	I/I1	FWHM (deg)	Intensity (Counts)	Integrated Int (Counts)
1	23.0200	3.86040	6	0.80000	7	421
2	25.9266	3.43383	26	0.61330	31	1028
3	28.2200	3.15976	7	0.20000	9	164
4	29.0250	3.07393	11	0.89000	13	575
5	31.0600	2.87701	19	0.60000	23	939
6	32.0200	2.79291	100	1.21600	121	6131
7	33.0200	2.71058	52	0.92000	63	2576
8	33.9000	2.64220	20	1.00000	24	1360
9	39.6900	2.26908	17	1.22000	21	1448
10	45.1400	2.00697	4	0.16000	5	66
11	46.8100	1.93919	20	1.02000	24	1369
12	47.8400	1.89981	10	0.00000	12	0
13	49.5650	1.83766	24	0.95000	29	1943
14	50.4000	1.80915	14	0.00000	17	0
15	51.2600	1.78080	12	1.84000	14	1290
16	53.1650	1.72139	12	0.65000	15	506
17	55.7400	1.64782	4	0.08000	5	72
18	60.0100	1.54037	3	0.38000	4	119
19	62.7700	1.47911	3	0.26000	4	101
20	64.0300	1.45301	11	0.82000	13	601
21	64.9000	1.43562	7	0.88000	8	360
22	71.9500	1.31130	4	0.18000	5	170
23	74.1400	1.27789	4	0.48000	5	240

Perhitunga ukuran kristal dengan rumus *Debye Scherer*

	2 theta (deg)	2 theta (rad)	theta	k	Wavelenght (nm)	FWHM (deg)	FWHM (rad)	cos theta	D	
30 Menit	26.0250	0.4542	0.2271	0.9	0.154	0.6900	0.0120	0.9743	11.812	9.242
	32.3266	0.5642	0.2821	0.9	0.154	1.6667	0.0291	0.9605	4.961	
	39.8400	0.6953	0.3477	0.9	0.154	1.3200	0.0230	0.9402	6.399	
	46.8900	0.8184	0.4092	0.9	0.154	0.9800	0.0171	0.9174	8.832	
	49.6000	0.8657	0.4328	0.9	0.154	0.9600	0.0168	0.9078	9.112	
	53.3300	0.9308	0.4654	0.9	0.154	0.6200	0.0108	0.8936	14.333	
60 Menit	25.9266	0.4525	0.2263	0.9	0.154	0.6133	0.0107	0.9745	13.287	9.726
	32.0200	0.5589	0.2794	0.9	0.154	1.2160	0.0212	0.9612	6.794	
	39.6900	0.6927	0.3464	0.9	0.154	1.2200	0.0213	0.9406	6.920	
	46.8100	0.8170	0.4085	0.9	0.154	1.0200	0.0178	0.9177	8.484	
	49.5650	0.8651	0.4325	0.9	0.154	0.9500	0.0166	0.9079	9.207	
	53.1650	0.9279	0.4640	0.9	0.154	0.6500	0.0113	0.8943	13.661	
60 Menit	26.0300	0.4543	0.2272	0.9	0.154	0.6200	0.0108	0.9743	13.146	10.234
	32.3700	0.5650	0.2825	0.9	0.154	1.5800	0.0276	0.9604	5.233	
	39.8800	0.6960	0.3480	0.9	0.154	1.0400	0.0182	0.9401	8.123	
	46.9350	0.8192	0.4096	0.9	0.154	0.8900	0.0155	0.9173	9.727	
	49.7100	0.8676	0.4338	0.9	0.154	0.9400	0.0164	0.9074	9.310	
	53.3000	0.9303	0.4651	0.9	0.154	0.5600	0.0098	0.8938	15.866	